JAERI-M
87-196

MULTI-MODE OPTICAL FIBERS FOR SIMULTANEOUS 13-POSITION MEASUREMENTS THOMSON SCATTERING APPARATUS IN THE JFT-2M TOKAMAK

November 1987

Toshihiko YAMAUCHI, Yoshiaki OGURA*, Ichiro NAKAZAWA**
and Tohru MATOBA

日本原子力研究所
Japan Atomic Energy Research Institute

JAERI-M レポートは，日本原子力研究所が不定期に公刊している研究報告書です。
入手の問合わせは，日本原子力研究所技術情報部情報資料課（〒319—11 茨城県那珂郡東海村）あて，お申しこしください。なお，このほかに財団法人原子力弘済会資料センター（〒319-11 茨城県那珂郡東海村日本原子力研究所内）で複写による実費頒布をおこなっております。

JAERI-M reports are issued irregularly.
Inquiries about availability of the reports should be addressed to Information Division, Department of Technical Information, Japan Atomic Energy Research Institute, Tokai-mura, Naka-gun, Ibaraki-ken 319-11, Japan.

編集兼発行　日本原子力研究所
印　　刷　山田軽印刷所

JAERI-M 87-196

Multi-Mode Optical Fibers for Simultaneous 13-Position Measurements Thomson Scattering Apparatus in the JFT-2M Tokamak

Toshihiko YAMAUCHI, Yoshiaki OGURA*
Ichiro NAKAZAWA** and Tohru MATOBA+

Department of Thermonuclear Fusion Research
Naka Fusion Research Establishment
Japan Atomic Energy Research Institute
Naka-machi, Naka-gun, Ibaraki-ken

(Received Octover 27, 1987)

The characteristics of fiber bundles for Thomson scattering optics are studied, whose fibers are made of multi-mode optical fibers. The variety of output patterns were observed by weighting on the fiber as well as by bending it after passing a He-Ne laser through a fiber bundle. This variety influenced the matching loss considerably. Then, the effect of former is larger than the latter, which is caused by the micro bending. And also, the spread of pulse width by weighting is connected with the spread of output pattern. The spread of pulse width was about 3ns at the most in a 2.3 m length of fiber bundle.

Keywords: Fiber Bundle, Thomson Scattering Optics, Multi-mode Optical Fiber, Output Pattern, Micro Bending

---

+ Department of Large Tokamak Research
* Sumita Optical Glass, Inc., Tokyo 105
** On leave from Mitsubishi Electric. Co., Tokyo 100

13点トムソン散乱装置用マルチモード光学ファイバー

日本原子力研究所那珂研究所核融合研究部
山内　俊彦・小椋　芳明*・中沢　一郎**・的場　徹+

（1987年10月27日受理）

トムソン散乱光学系に使われているマルチモードバンドルファイバーの諸特性が研究された。He－Neレーザー光をファイバーに通し，ファイバーの曲げに対してばかりでなく荷重を加えた時の光出力パターンの直径の変化を観測した。この変化はマッチングロスに重大な影響を与えた。この時，荷重による影響は曲げの影響より大きい。またこの荷重の影響はマイクロベンディングによって起きる事が判った。また，荷重による光パルス幅の広がりは光出力パターンの広がりと関係がある。長さ2.3 mのバンドルファイバーでは光パルス幅の広がりは最大3 nsである。

那珂研究所：〒311－02　茨城県那珂郡那珂町大字向山801－1
＋　臨界プラズマ研究部
＊　住田光学㈱
＊＊　三菱電機㈱

Contents

目　　次

1. Introduction

The Thomson scattering apparatus was reconstructed to measure 13 positions simultaneously from 6 positions in JFT-2M tokamak[1]. The main parts of reconstruction are the collecting lens (diameter of the first lense increases from 12 cm into 22 cm), fiber bundles (two sets or two times' scale than that of before channels), Littrow type spectrometers (two sets) and the data acquisition systems. In this paper, the fiber bundles were studied for transmitting the scattered signals effectively.

The optical fibers with core and cladding structure are generally classified into two types. One is called as "multi-mode optical fiber (MOF)" propagating the multi-mode light and the other is called as "single-mode optical fiber (SOF)" propagating the single-mode light. The main difference is derived from the core diameter, of which the former is 50∿200 μm and the latter is 5∿10 μm. The mode propagating through the latter is the lowest HE_{11} mode and the dispersion is very low compared with MOF. When the many modes are propagated in MOF, the pulse width becomes wider from their differences of group velocity. This width is given by $\tau=0.5n_1/c\times\sin^2\theta_{max}$, $\theta_{max}=\sin^{-1}((n_1^2-n_2^2)/n^1)^{1,2)}$. ($n_1$ and n_2: the refractive index and the subscripts 1 and 2 mean the core and cladding. c: the light velocity in free space.) This phenomenon is clearly measured by the plastic fiber (PF), in the case of value $n_2=0$, which is used as the optical fiber for the laser power monitor in our device. The gate duration to integrate the signal should be widened for that laser pulse. Moreover the study of spatial profile about these fibers is important to obtain the high transmittance. The study connected with MOF was extensively tried at the early stage of fibers development. Recently, the SOF has been studied for the optical fiber communication mainly. Thus MOF is not used for the optical fiber communication but for the effective transport of light. That is, the image optical fiber and the optical fiber bundle are constructed by MOF. For example, the optical fiber bundle is used for transmitting the scattered light obtained by Thomson scattering experiment[1]. When the MOF is used for the relay optics of Thomson scattering device, the followings are significant; First, to raise the packing ratio of MOF (Method: use the fiber as thick as possible and force the fiber bundle). Second, to decrease the transmission loss (use the fiber as short as possible and hold the incident angle as small as possible). Third, to match the fiber bundle with the

collecting lens and spectrometer composing the device (adjust the matching angle). The multi-mode optical fiber of this device has the value of 0.59 in the numerical aperature and matches to the other optics. But the shape at the end of fiber bundle is a rectangle. When some multi-mode optical fibers are packed into a rectangle metal case, some weight is supplied to increase the packing ratio. However, the divergence of output light becomes large by weighting on the fiber and it leads to bad matching with other optics. For those phenomena this study was performed in connection with the MOF or the fiber bundle. This stress-applying effect was studied in SOF for the manufacture of "polarization-maintaining" SOF[4]. There, the SOF has a circular core at the center of the fiber, just as in standard single-mode fibers, but it has axially nonsymmetrical "stress-applying" parts that are highly doped with a material such as boron. But, as the cladding of MOF is very thin in this apparatus, the force was directly applied to study that effect.

The MOF used for Thomson scattering device is 50 μm in diameter. But the thick silica glass fibers are used for the other Thomson scattering devices which are generally called as TVTS (multichannel Thomson scattering system with TV tube) in PLT[5] and DIII[6] tokamaks. Their diameter of MOF is 200 μm. The larger is diameter of MOF, the better does transmission become. The polarization characteristics was also measured. As described in ref.7, the polarized light became the unpolarized light after passing through a fiber.

The varieties of output pattern using He-Ne laser light are observed by weighting on the fiber bundle from side as well as by bending them. In chapter 2 the experimental arrangement is described and the characteristics affected by weighting and bending are described in chapter 3. The spread of pulse width by weight is described in chapter 4, using the heterostructure laser. The fiber bundle reconstructed for the Thomson scattering device is explained in chapter 5, and the conclusion is presented in chapter 6.

2. Experimental Arrangement

Figure 1 shows the experimental arrangement. As light sources, a He-Ne laser (or in some cases heterostructure laser with single-mode) with both multi-mode and unpolarization was used as shown in Fig. 1. Laser light is incident on the input end of some fibers at the angle θ. The area of their input end is large compared to the diameter of He-Ne laser. The kinds of optical fibers used here are listed in Table I, which are a silica glass, a multi-component glass and a plastic fibers. The diameter of fiber bundle made of the multi-component glass fiber, which is used for 13-position measurements Thomson scattering apparatus, is 6.5 mm^{ϕ} to the diameter 1 mm^{ϕ} of He-Ne laser.

This fiber is 230 cm long, and the weighting and the bending action was performed in the middle of the fiber. The pattern of output light was drawn on the screen as shown in Fig. 1, whose ring pattern was obtained by the oblique incidence of laser light.

Table 1 Physical characteristics of three kinds of optical fibers.
$(2\alpha/\beta)$max : maximum receiving angle

Fiber	Diameter	Core(1)	Cladding(2)	n(1)	n(2)	N. A.	$(2\alpha/\beta)_{max}$
Silica	200 μm	190 μm	10 μm	1.43	1.38	0.38	45 deg
Glass	50	45	5	1.62	1.51	0.59	72
Plastic	500	470	30	1.49	1.40	0.52	63

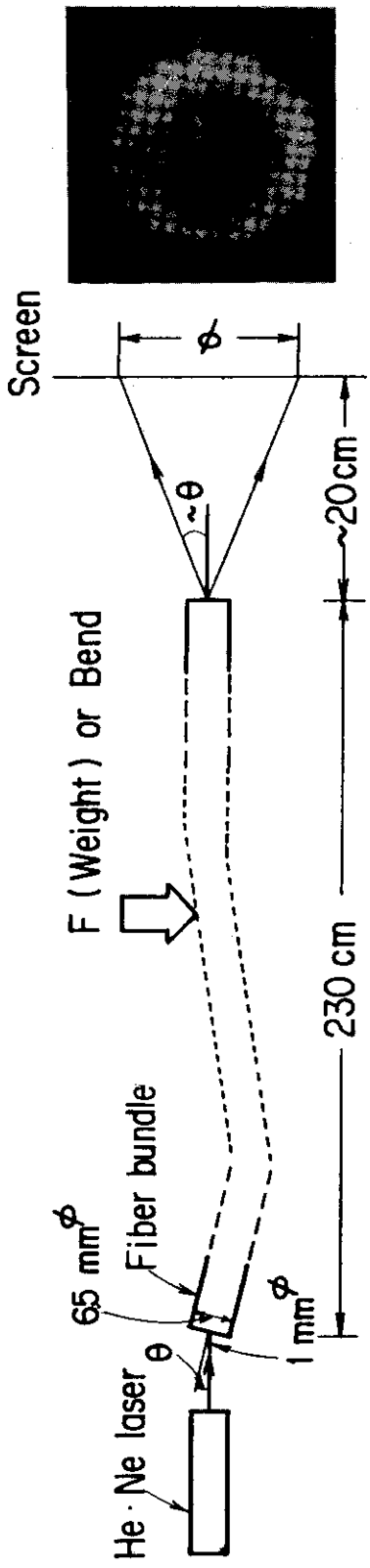

Fig. 1 Experimental arrangement for fiber experiment.

3. Experimental Result

The near field pattern (NFP) and the far field pattern (FFP) of multi-component glass fiber obtained by the incidence of He-Ne laser are shown in Fig. 2(a) and (b), respectively. As a He-Ne laser is 1 mm$^{\phi}$ in diameter, the output end of fibers (shown by "No signal") are also found in Fig. 2(a) as well as the speckle patterns by the weak incident light are found on the surface (shown by "NFP"). These speckle patterns move around on the surface by soft touching, which seems to be derived from the change of light path, caused by micro bending in the core. The NFP of speckle pattern at the up and middle in Fig. 2(a) is derived from the interferences among some modes on the output end since the pattern of input light is nearly uniform intensity on the input end with coherent. The FFP in Fig. 2(b) shows the multi-mode, which is apparently found in the rotational direction like a petal.

The output patterns with weight and without weight are shown in Fig. 3, when the Ne-Ne laser is incident on the input end at $\theta=0°$ and $10°$. By weighting on the fiber the light comes out in the edge region at $\theta=0°$ and the central region at $\theta=10°$. (However, it is found that the radius of the pattern becomes large after the light being filled in the central region at $\theta=10°$) This is based on the fact that the higher-mode light traveling in the fiber changes into the lower-mode light. On the contrary, the circular pattern of lower-mode light at the incidence $\theta=0°$ becomes larger circular pattern by weighting on it. That is, some lower-mode lights change into the higher-mode lights. The diameter of pattern at the incidence angle $\theta=0°$ is shown in Fig. 4 as the function of weighting. That diameter increases in proportion to the wight from the initial value $\phi_p=55$ mm. The spatial profile of output light from fiber at the incidence angle $\theta=0°$ is shown in Fig. 5. It is found from Fig. 5 that the lower-mode within the radius $0.9\sim1.3$ cm changes into higher-mode. The spatial profile of output light from fiber at the incidence angle $\theta=10°$ is shown in Fig. 6. As already shown in Fig. 3, the diameter of this pattern in constant, but the light intensity in the central region becomes 1.7 times higher than that of weight $P=0$ kg. Therefore, figure 7 is picturized based on the above results. The upper figure shows the ring pattern and the lower figure shows the circular pattern. In these figures, the pattern changes into the right direction as arrows by weighting. The spread angle inside the output end is given

by[1)]

$$\theta^c = m\lambda/4an_1 = 4.3 \times 10^{-3} \times m \qquad (1)$$

Where m is the group of LP (linearly polarization) mode number, λ the wavelength (6328 Å) in the free space, a the core radius (22.5 μm) and n_1 the refractive index of the core (1.62). Using eq.(1) the mode number increases from $2\times m$=60 to 80 with the correlation to the weight from P=0 Kg to 5.5 Kg. Here, the stress seems not to affect the refractive index n_1 uniformly but the refractive index distribution ununiformly just as SOF. From eq.(1) it is understood that the core diameter should be large for the decrease of dispersion angle as well as for the increase of packing ratio.

The bending the fiber bundle was tested to compare with the above mechanism. The change of output pattern in diameter is shown in Fig. 8 as a function of the bending radius, which is obtained by bending the fiber bundle at the position F in Fig. 1. The minimum bending radius is 2 cm, which is much larger than the core diameter. The increment of radius is 16% in this case, and even if the bending radius is 10 cm, it is only 9%. Thus the mode change is less than that of above result.

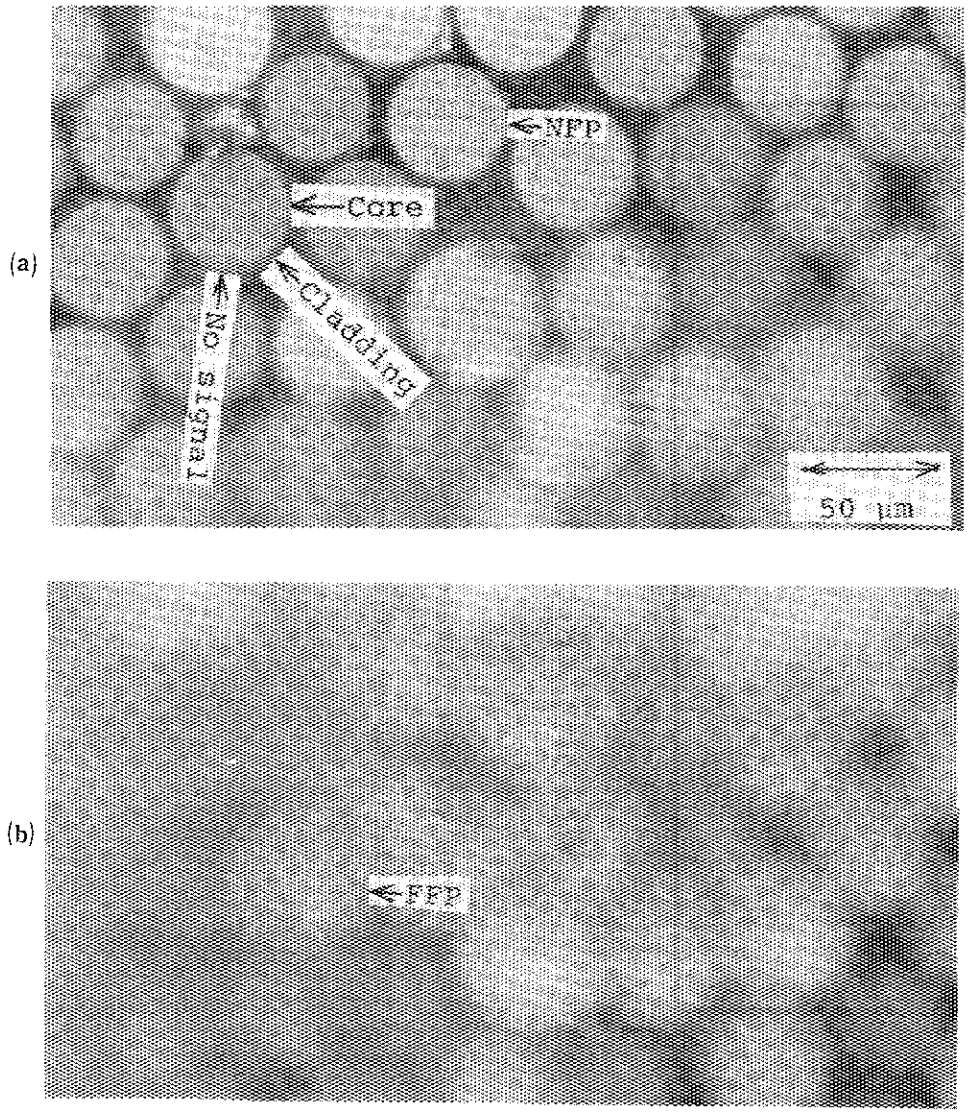

Fig. 2 Output patterns from the fiber bundle using multi-component glass fiber (×100).
(a) near field pattern (b) far field pattern

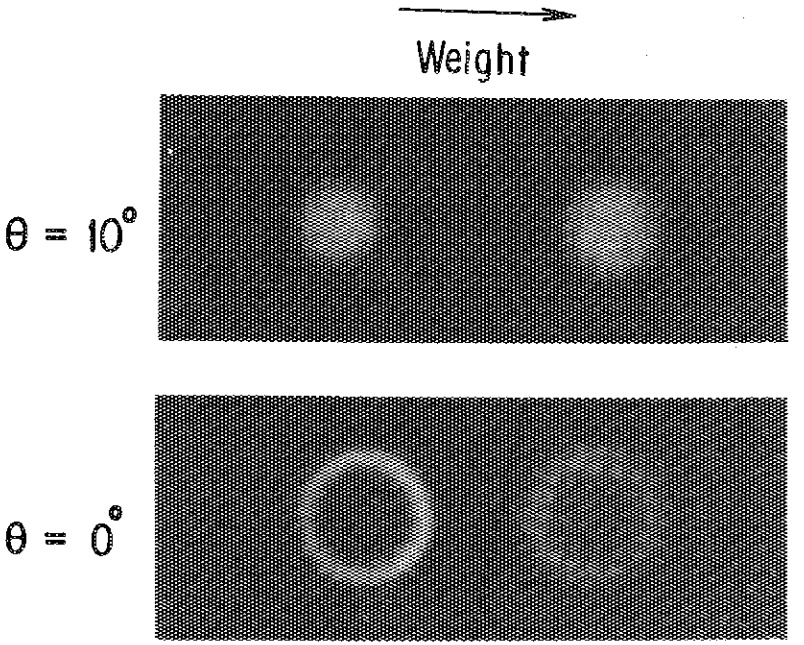

Fig. 3 Variety of pattern by weighting on the fiber bundle using He-Ne laser.

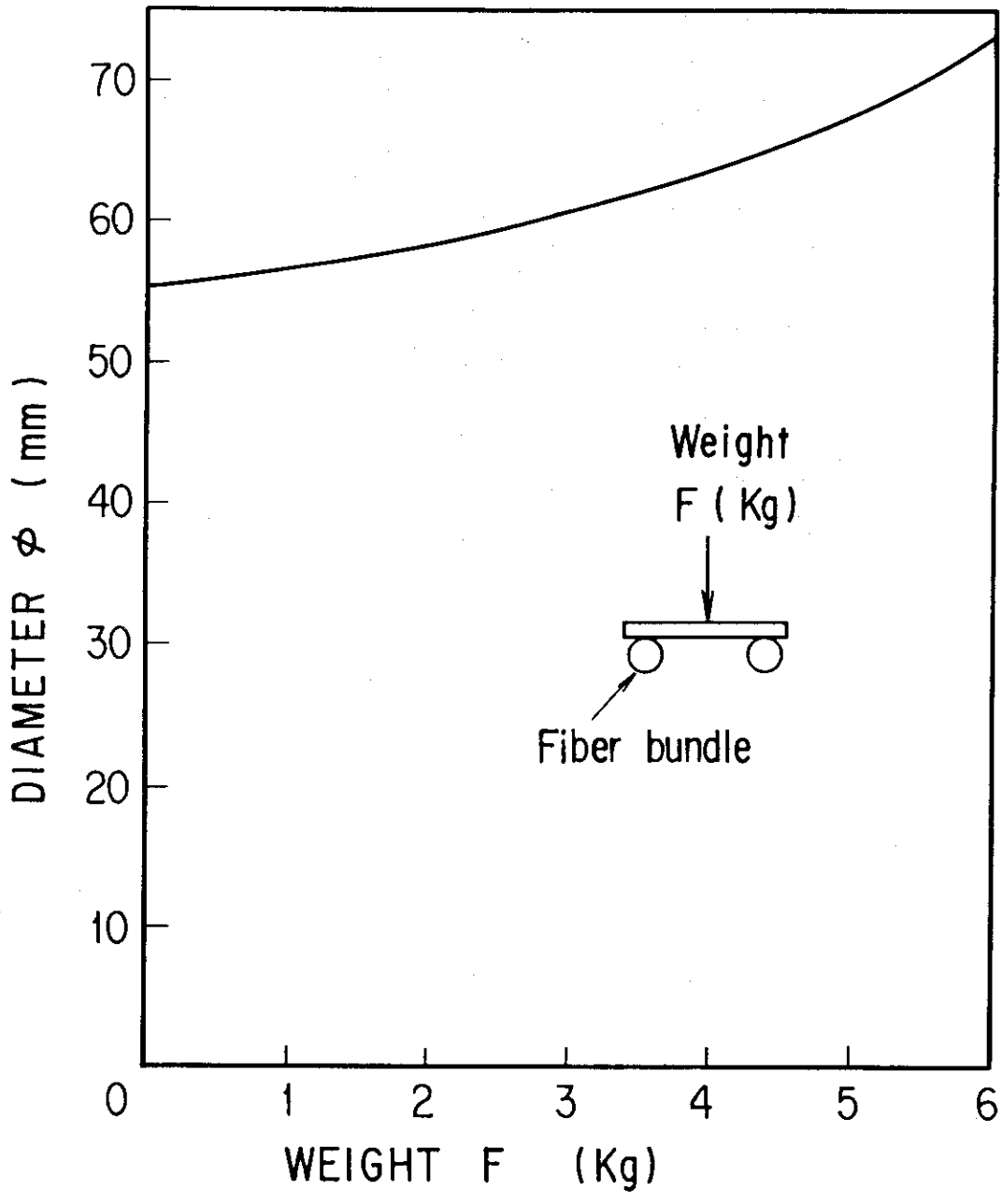

Fig. 4 Increase of pattern diameter by weighting on the fiber bundle.
loaded length : 80 mm and distance between fibers : 80 mm.

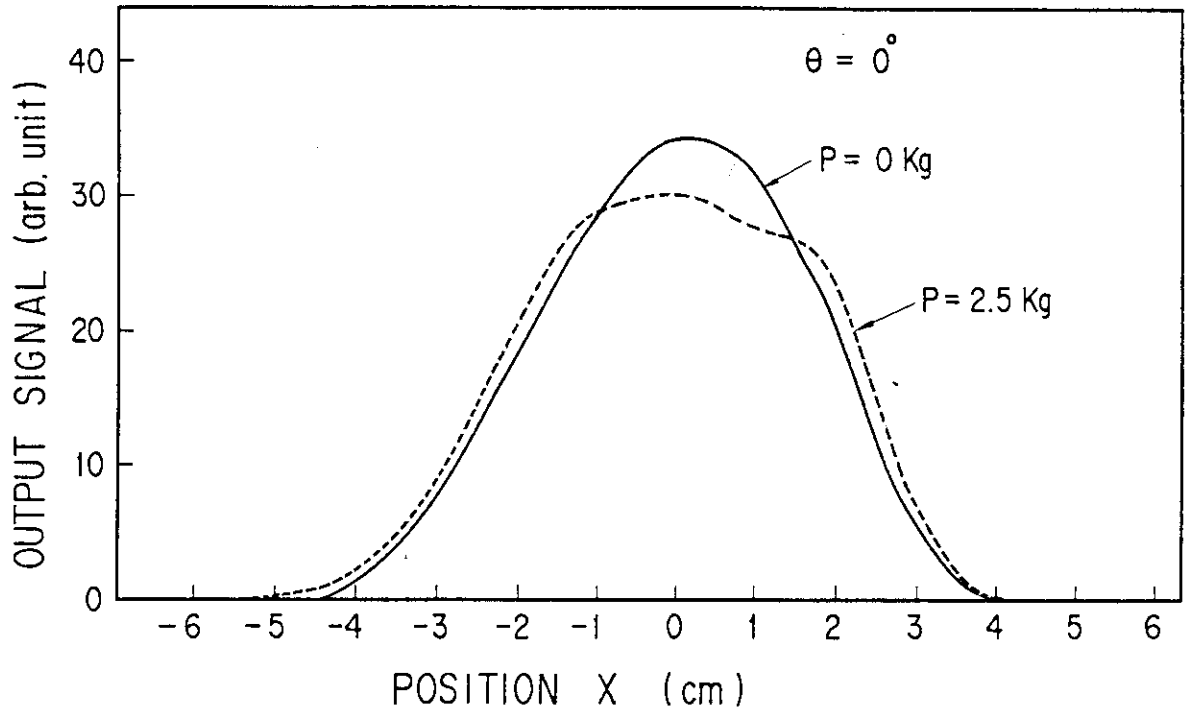

Fig. 5 Pattern profile by weighting on the fiber bundle. (θ = 0°).

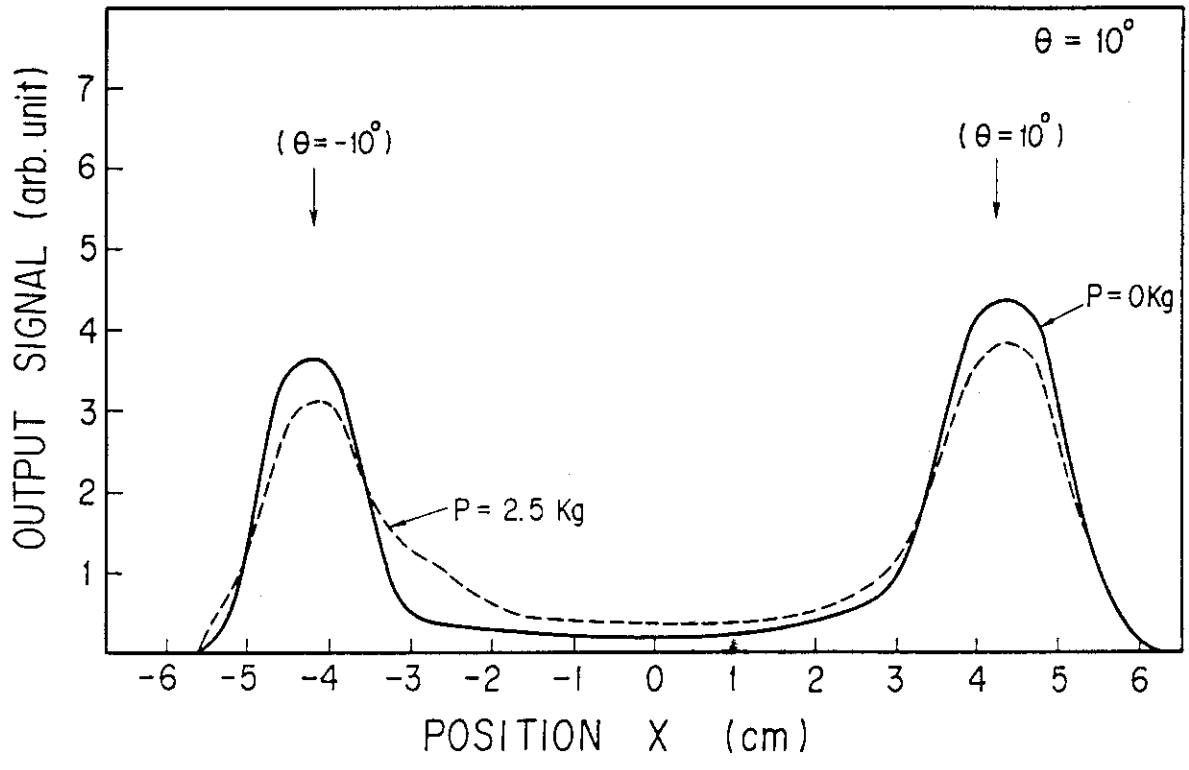

Fig. 6 Pattern profile by weighting on the fiber bundle. (θ = 10°).

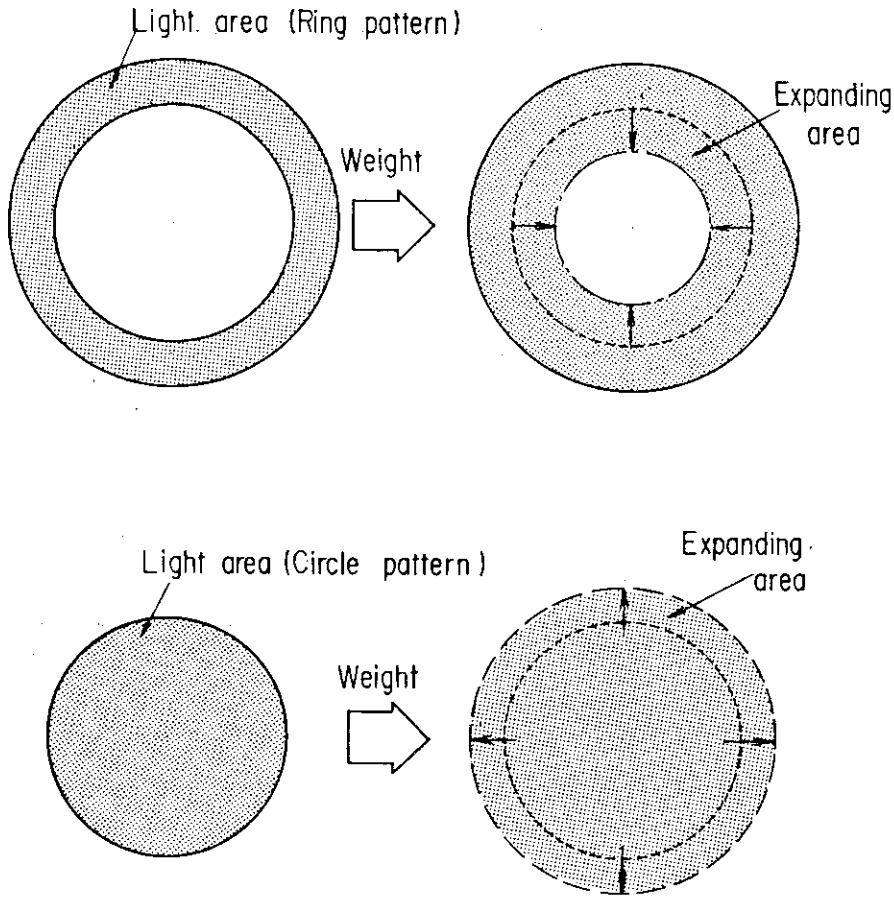

Fig. 7 Output patterns by weighting on the fiber bundle.

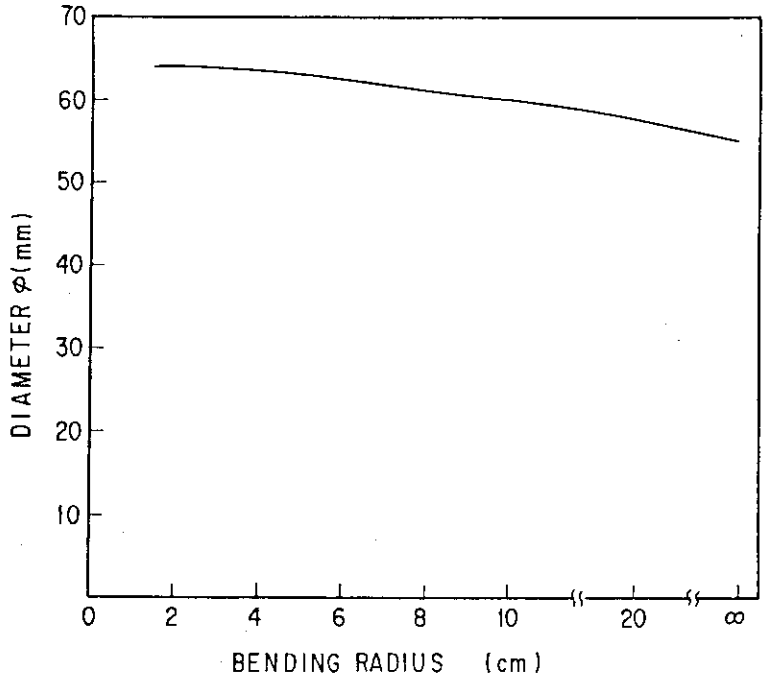

Fig. 8 Increase of pattern diameter by bending the fiber bundle.

4. Spread of Pulse Width

The spread of pulse waveform by the fiber is affected by not only n_1 in core but also the fiber length L. It is considered as the time difference between the straight path and the reflective path in the fiber, as the scattered light is collected through the F=2 lens. That is, the time required to propagate through the fiber length L is

$$\tau_\theta = n_1 L/(c \times \cos\theta^c) = \tau/\cos\theta^c \qquad (2)$$

This equation represents the transit time in the small incident angle is shorter than that in the large incident angle. Therefore, the pulse width should be broadened when the output light from the fiber is gathered on a detector as $\sum_{\theta^c=0}^{\theta} \tau_\theta$. The averaged spread of pulse width is given by

$$\bar{\tau}_w = \frac{\sum_{\theta=\theta^c} (\tau_\theta - \tau)\, f(\theta)\, \Delta\theta}{\sum_{\theta=\theta^c} f(\theta)\, \Delta\theta} \qquad (3)$$

where $f(\theta)=I_o r_o^2 \times (1-\tan\theta/\tan\theta_o) \times \tan\theta/(\cos^2\theta \times \tan^2\theta_o)$ is the spatial intensity distribution on the input end emitted from heterostructure laser called as FFP, and I_o is the peak value in the triangular shaped profile of heterostructure laser beam, θ_o the maximum incident angle (35°) and r_o the distance between a light source and the fiber bundle and $\Delta\theta$ the infinitely small angle. For this consideration, the experiment using heterostructure laser (λ=7800 Å) is performed, and this heterostructure laser is position at the place of He-Ne laser in Fig. 1. The photomultiplier (PM) obtained by PM tube is shown in Fig. 9. This figure shows the input waveform, the output waveform after passing through the fiber at the normal incidence using heterostructure laser and the control voltage signal (C.S.) applied into this laser. The experimental transit time is 13ns which agrees with that estimated from $n_1 L/c$=12ns. The averaged spread of pulse width using this laser is 0.5ns, calculated from eq.(3) at the incidence angle θ=0° and the angle of radiating light θ=33°. At the incidence angle θ=30°, the experimental spread of pulse width is 1-3 ns which agrees with the estimated value 1.9ns from eq.(3). The experimental value of pulse spread (•) is shown in Fig. 10 with the

theory. The experimental value seems to be slightly larger than the theory because the light does not pass through on a plane but rotating in core. In addition, when weight P=4 Kg is putting at the distance 10 cm from the input end, the pulse width becomes large slightly at a normal incidence. This fact means the change of reflective direction caused by the micro bending, which is corresponding to the result of § 3. It seems that this produces an anisotropic refractive index distribution in the core region, but the degeneration of light intensity is not observed just as SOF.

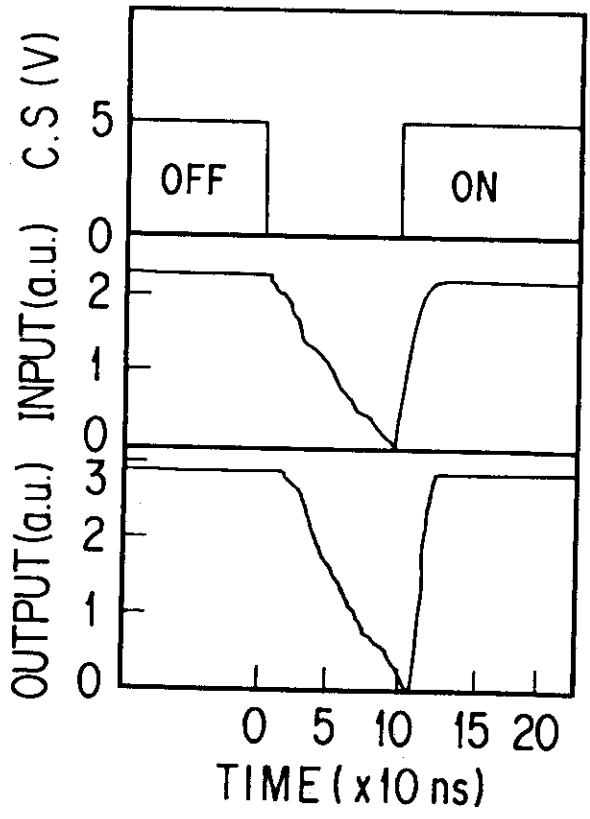

Fig. 9 Output waveform from the fiber bundle at the normal incidence.

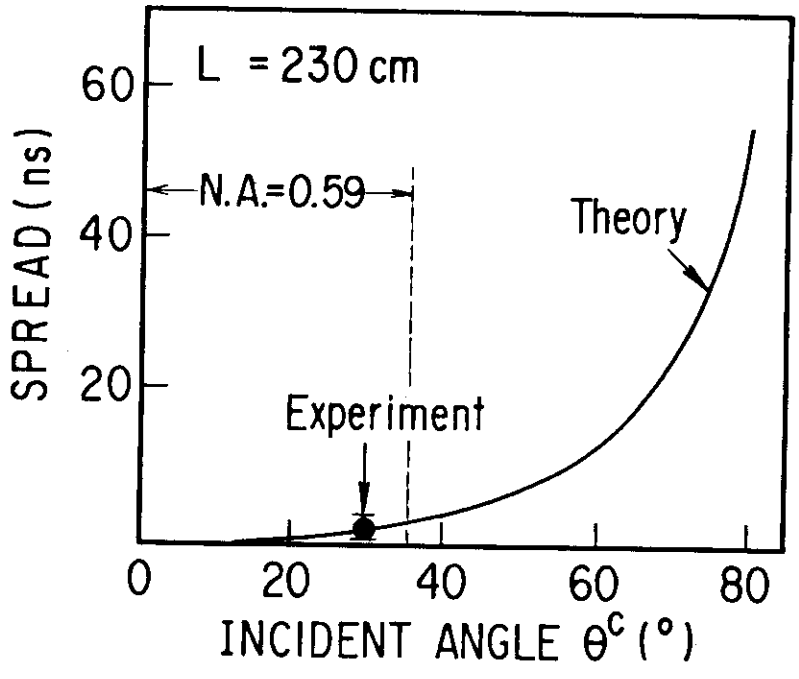

Fig. 10 Time spread of pulse width connected to the incident angle θ^c in core.

5. Construction of Fiber Bundle for Thomson Scattering Device

Recently, as the reliability of fiber has increased much high, it has been used at the position between collecting lens and spectrometer as well as at the position between spectrometer and PM tube. For this improvement, the light path length between collecting lens and spectrometer decreased from ∿2 m to below ∿1 m and then the apparatus became compact. One optical path from a scattering point to PM tube is shown schematically in Fig. 11. When a large lens (diameter : 12 cm → 22 cm, F number : 2 at the center) is used for collecting the scattered light with the large solid angle, a fiber of large numerical aperature need to be used for a correct matching. The field lens transmits the light which is incident from the fiber bundle into the Littrow lens, which two Littrow type spectrometers are used for measurement of 13 points vertically. The fiber bundle used here is flexible. However, those in PLT and DIII are rigid, which is made with silica glass and the large diameter 200 μm. The flexible type used here is very convenient to change measuring positions and spectral channels. (by exchanging fibers or moving the collecting lens in a vertical line). The first fiber bundle is shown in Fig. 12(a) and the second fiber bundle is shown in Fig. 12(b). As shown in Fig. 12(a), the number of measuring points in tokamak plasma are 13. The cross-section of each input end is rectangle and that of output surface is an arc whose length and width are 70 mm and 3 mm, respectively, which is larger than the one described in ref. 1. The 13 points are separated into two sections. One is the fiber bundle to measure the 7 points (central high temperature region) and another is the 6 points (edge low temperature region) as the slit length in spectrometer is restricted within 70 mm. To reduce the loss light the thin glass plates with anti-reflective coating are adhered on the both surfaces of fiber bundles. The length of fiber is designed as short as possible not to lose the scattered light. The transparent type of PM tube having a large photoelectric surface is easy to match between them compared to the reflective type. The matching lenses are used for matching with the photoelectric surface of reflective type of PM tube described in ref. 1.

The loss, by weighting at the part the fiber bundle connects to the spectrometer, is caused by the increment of divergence from the output end of first fiber bundle in Fug. 11. (When second fiber bundle is

connected with PM tube with a large photoelectric surface, it is no problem) The output area of fiber bundle is small compared with that of field lens. That is, the maximum loss ratio L_{MAX} is given by

$$L_{MAX} = (S^* - S)/S = \tan(\alpha/\beta + \gamma)/\tan(\alpha/\beta) - 1 \qquad (4)$$

where S and S^* represent the original area on the field lens and the expanding area by weighting, respecively. α/β and γ are a half of the solid angle incident on the fiber bundle from the collecting lens and a half of the solid angle of incremental divergence from the output end, respectively. β is the magnification of collecting lens. The incremental width of output light from the fiber bundle is considered for the loss ratio because the vertical length of this rectangular lens is long compared to the width. For example, using Fig. 4, the total loss ratio reaches at

$$L_{MAX} = 0.25 \qquad (5)$$

where $\alpha/\beta=8°$ and $\gamma=2°$ corresponding to the diameter ϕ_p= 55 mm and the incremental diameter $\Delta\phi$=15 mm in Fig. 4, respectively and β=0.4. This value is a half of the transmittance measured using the fiber bundle.

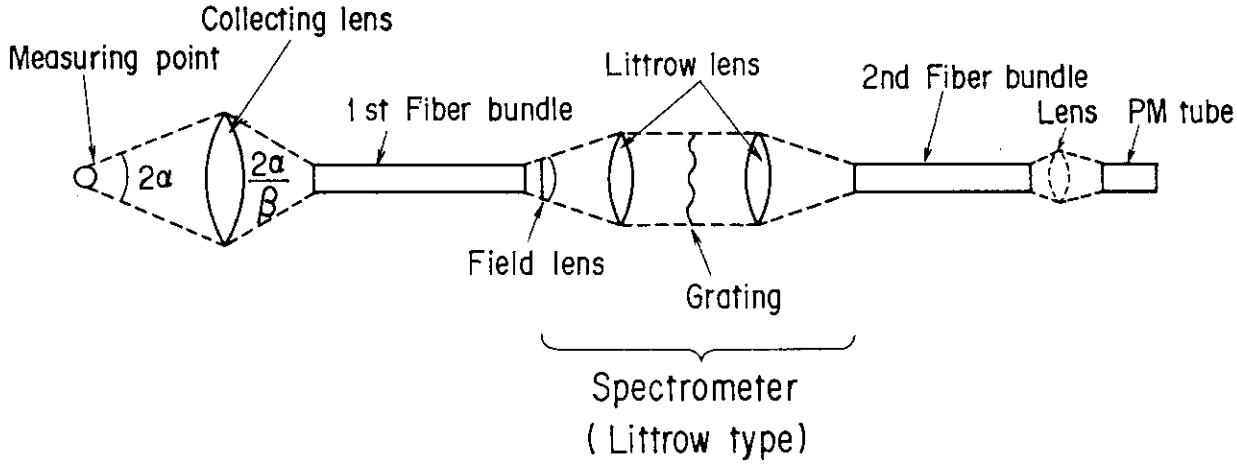

Fig. 11 Optical path diagram in Thomson scattering device.
β : magnification

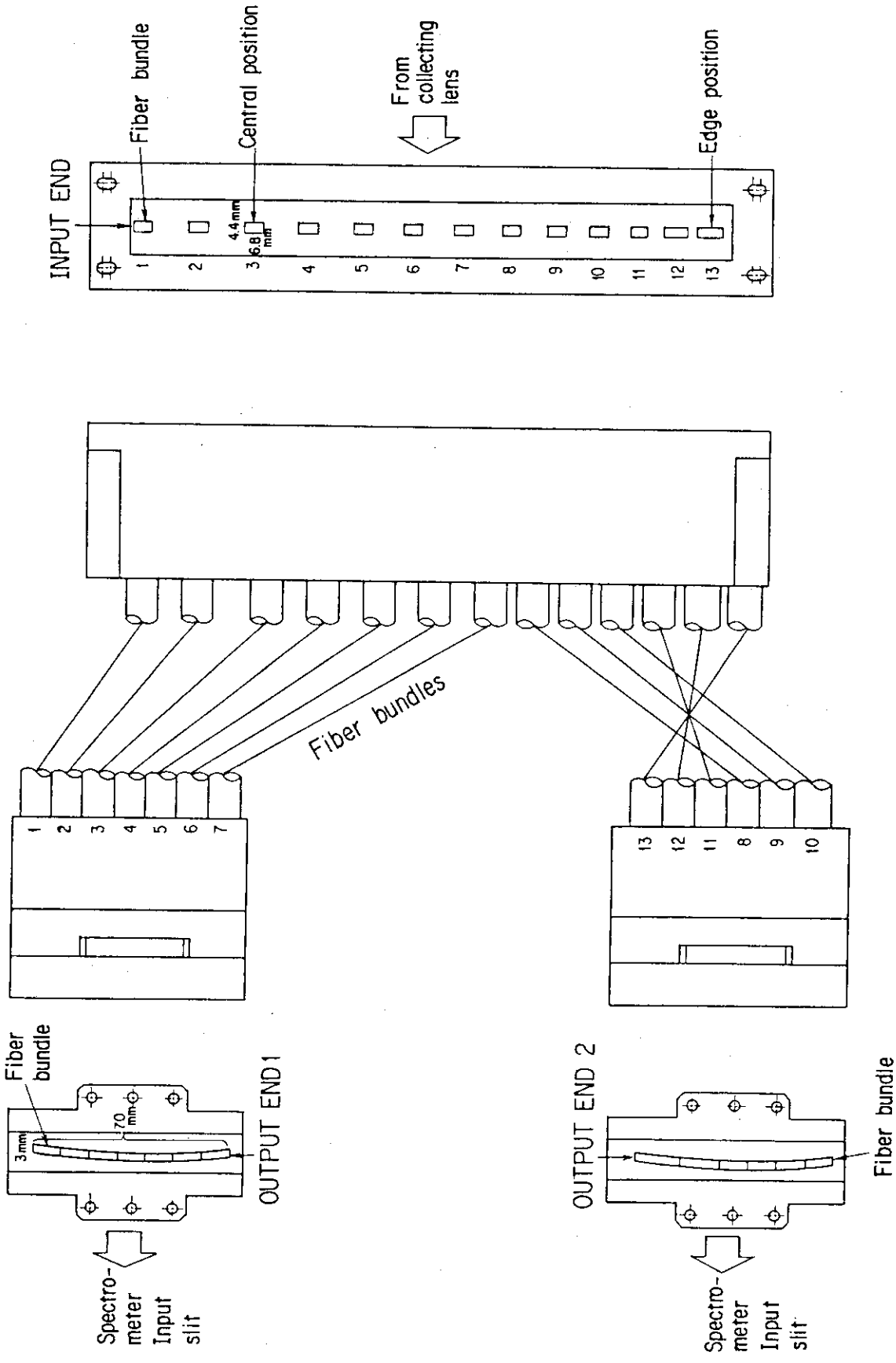

Fig. 12 Fiber bundle constructed for Thomson scattering device.
(a) for between a collecting lens and a spectrometer

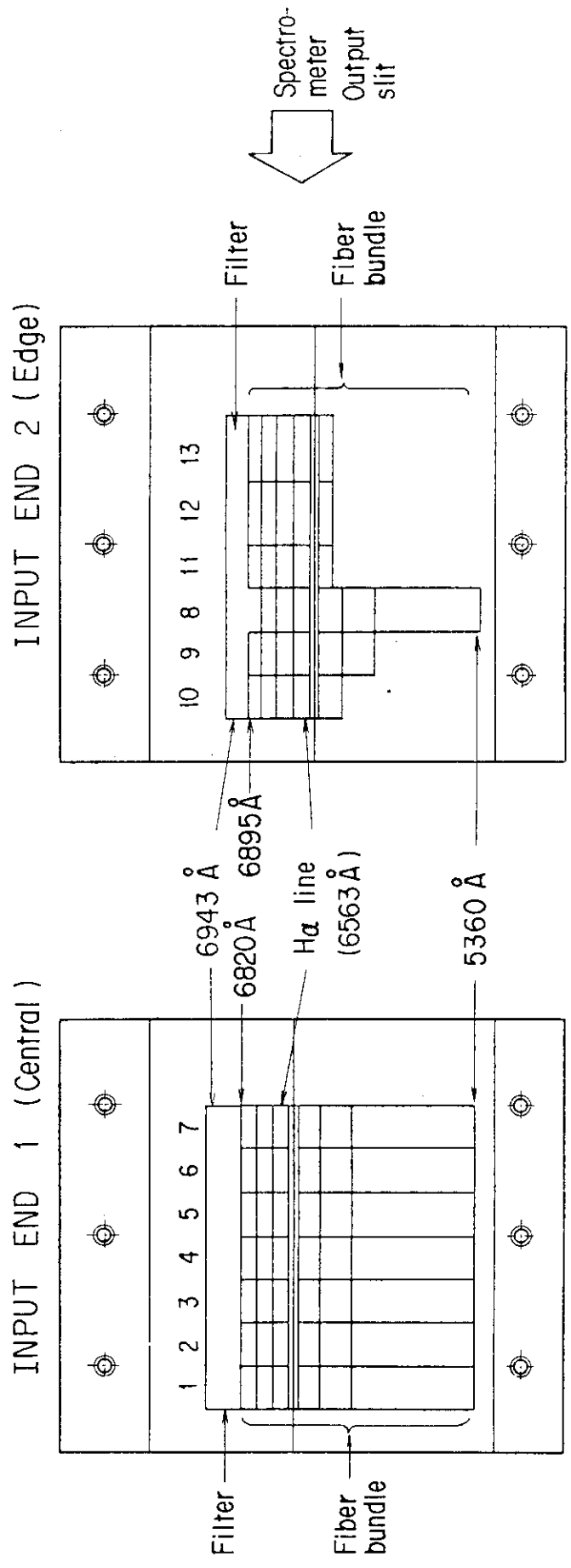

Fig. 12 (continue)
(b) for between a spectrometer and PM tubes.

6. Discussion and Summary

Thomson scattering apparatus was reconstructed for measuring 13 points simultaneously from that in ref.1. All components except for ruby laser, PM tubes and mini-computer were reconstructed. As the results of this reconstruction, the apparatus resolves 13 spatial positions separated by a distance of about 5 cm. 4-5 wavelength elements allows temperature measurement in the range ∿50eV to ∿5KeV. (Z=-10 cm to Z= 50 cm).

The characteristics of the multi-component glass fiber is measured using the coherent light spatially and then in this paper the characteristics the fiber bundle for Thomson scattering are described. It is found that the incremental divergence of the output light from the fiber by weighting is small till 1 Kg, but the transmission ratio by weighting decreases. The incremental divergence to the bending is much smaller than that of the weighting.

The transit time of pulse being incident on the fiber bundle at small angle(lower mode) is shorter than that at large angle (higher mode). The spread of pulse width after passing through the fiber bundle is found to be the change of mode number caused by the micro bending. (The input light with large divergence becomes the large pulse width.) This weighting or stress is caused by micro bending, which produces an anisotropic refractive index distribution in the core region[4].

As it is found from geometry that the larger is the diameter of fiber, the higher does the transmission ratio become, using the multi-component glass fiber of diameter 250 μm the fiber bundle is constructed experimentally.

1) Output pattern is changed by weighting as well as bending.
2) Output pattern is changed by weighting larger than bending, which is caused by micro bending.
3) Spread of pulse width corresponds to change of output pattern.

The 13-position measurements Thomson scattering apparatus has been taking a data in JFT-2M tokamak. The differences or causes of H-mode and L-mode discharges will be clearized, as the relation between sawtooth oscillation and electron energy profiles has been studied from this measurement and so on[8].

Acknowledgement

The authers would like to express their thanks Drs. S. Kasai, N. Suzuki and K. Suzuki for their contineous support. In addition, they wish to thank Drs. H. Maeda, A. Funahashi, Y. Tanaka, M. Tanaka, K. Tomabechi and S. Mori for their continuous encouragement.

References

1) T. Yamauchi, K. Sano, H. Kawashima, K. Kumagai and T. Matoba, Jpn. J. Appl. Phys. 21 (1982) 347.
2) T. Okoshi, K. Okamoto and K. Hotate, "*Optical fibers*," Ohm Press (1983) [Japanese].
3) Obshansky, R. and Keck, D.B., Appl. Opt. 15 (1976) 483.
4) M. Nishimura, "Photonics Spectra," Ed. Teddi C. Laurin, June (1986) 109.
5) N. Bretz, D. Dimock, V. Foote, D. Johnson, D. Long and E. Tolnas, Appl. Opt. 17 (1978) 192.
6) D. Vaslow, G. Hsieh and J.R. Smith, Bull. Am. Phys. Soc. 27 (1982) 959.
7) T. Yamauchi and I. Yanagisawa, Jpn. J. Appl. Phys. 24 (1985) 1528.
8) T. Yamauchi, T. Shoji, S. Yamamoto and N. Suzuki, Jpn. J. Appl. Phys. 26 (1987) 1117.
T. Yamauchi, T. Shoji and S. Yamamoto, to be published in Plasma Phys. and Contr. Fusion (1987)

Acknowledgement

The authers would like to express their thanks Drs. S. Kasai, N. Suzuki and K. Suzuki for their contineous support. In addition, they wish to thank Drs. H. Maeda, A. Funahashi, Y. Tanaka, M. Tanaka, K. Tomabechi and S. Mori for their continuous encouragement.

References

1) T. Yamauchi, K. Sano, H. Kawashima, K. Kumagai and T. Matoba, Jpn. J. Appl. Phys. 21 (1982) 347.
2) T. Okoshi, K. Okamoto and K. Hotate, "*Optical fibers*," Ohm Press (1983) [Japanese].
3) Obshansky, R. and Keck, D.B., Appl. Opt. 15 (1976) 483.
4) M. Nishimura, "Photonics Spectra," Ed. Teddi C. Laurin, June (1986) 109.
5) N. Bretz, D. Dimock, V. Foote, D. Johnson, D. Long and E. Tolnas, Appl. Opt. 17 (1978) 192.
6) D. Vaslow, G. Hsieh and J.R. Smith, Bull. Am. Phys. Soc. 27 (1982) 959.
7) T. Yamauchi and I. Yanagisawa, Jpn. J. Appl. Phys. 24 (1985) 1528.
8) T. Yamauchi, T. Shoji, S. Yamamoto and N. Suzuki, Jpn. J. Appl. Phys. 26 (1987) 1117.
T. Yamauchi, T. Shoji and S. Yamamoto, to be published in Plasma Phys. and Contr. Fusion (1987)